

# High-Fidelity Quantum Information Transmission Using a Room-Temperature Nonrefrigerated Lossy Microwave Waveguide

Montasir Qasymeh\*

*Electrical and Computer Engineering Department  
Abu Dhabi University, Abu Dhabi, UAE* †

Hichem Eleuch

*Department of Applied Physics and Astronomy  
University of Sharjah, Sharjah, UAE and  
Institute for Quantum Science and Engineering  
Texas A&M University, Texas, USA*

(Dated: November 30, 2021)

Quantum microwave transmission is key to realizing modular superconducting quantum computers [1] and distributed quantum networks [2]. A large number of incoherent photons are thermally generated within the microwave frequency spectrum. Hence, high-fidelity quantum microwave transmission has long been considered to be infeasible without refrigeration [3, 4]. In this study, we propose a novel method for high-fidelity quantum microwave transmission using a room-temperature lossy waveguide. The proposed scheme consists of connecting two cryogenic nodes (i.e., a transmitter and a receiver) by the room-temperature lossy microwave waveguide. First, cryogenic preamplification is implemented prior to transmission. Second, at the receiver side, a cryogenic loop antenna placed inside the output port of the waveguide is coupled to an *LC* harmonic oscillator located outside the waveguide. The loop antenna converts quantum microwave fields (which contain both signal and noise photons) to a quantum voltage across the coupled *LC* harmonic oscillator. Noise photons are induced across the *LC* oscillator include the amplification noise, the thermal occupation of the waveguide, and the fluctuation-dissipation noise. The loop antenna detector at the receiver is designed to extensively suppress the induced noise photons across the *LC* oscillator to effectively cool the waveguide. We show a suitably designed preamplification gain can be used in conjunction with the loop antenna at the receiver to realize high-fidelity quantum transmission (i.e., more than 0.97) over distances up to 100 m.

## I. INTRODUCTION

Realizing large-scale quantum computers with thousands (or millions) of qubits requires efficient quantum data transmission between distant quantum nodes [5–7]. This architecture of remotely connected quantum modules is known as a modular quantum computer [8], which has been purported as a means of overcoming the current challenges that prevent the scale-up of quantum computers, such as crosstalk, input/output coupling limitations, and limited space [9, 10]. Likewise, future quantum sensing applications and networks require efficient quantum transmissions with applicable implementations [11–15]. Among the main quantum technologies that have been developed, superconducting-based quantum circuits have shown exceptional potential for quantum signal processing and computation [16–18]. However, superconducting signals operate in the microwave frequency spectrum and are therefore particularly vulnerable to degradation by thermal energy. Therefore, superconducting circuits are typically housed in cryostats. This operating condition imposes strict limitations on the ability to build modular superconducting quantum computers. Several

approaches have been proposed to connect distant superconducting quantum circuits. One approach is based on entangling distant superconducting circuits using coaxial cables carrying microwave photons [19–21] or acoustic channels carrying phonons [22]. Transmission lengths between 1 and 2 m have been reported using this technique. Another approach involves cooling a microwave waveguide to cryogenic temperatures [3]. Five meter coherent microwave transmission was reported. These two approaches require housing transmission channels to be placed in dilution refrigerators, which is challenging in terms of both economy and implementation. In this regard, IBM has announced plans to build a jumbo liquid-helium refrigerator, 10 feet tall and 6 feet wide, to support a 1000 qubit quantum computer that is planned for construction in 2023 and a milestone million qubit quantum computer that is planned for construction in 2030 [23]. In [24, 25], quantum information transmission via noisy channels was proposed using a time-dependent coupling between qubits (at the transmitter and receiver) and a connecting channel. However, channel loss and dissipation-generated noise were not taken into account. This approach requires operating at a few Kelvins (i.e., 4 K) and implementing quantum-error correction to attain high-fidelity transmission. Other researchers have proposed alternative approaches in which optical fibers are used to connect superconducting cryogenic circuits (or processors), facilitated by microwave-to-optical trans-

\* montasir.qasymeh@adu.ac.ae

† <http://www.montasir.qasymeh.com>

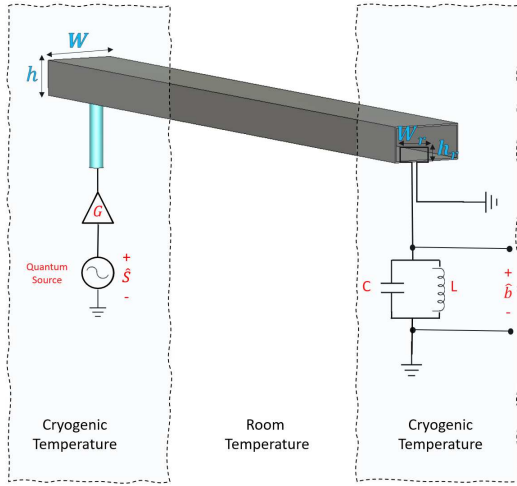


FIG. 1. Proposed system for microwave transmission using a room-temperature waveguide.

duction [4, 26–28]. However, several challenges remain in realizing efficient wide-band electro-optic transducers, and drawbacks are associated with transduction resulting from the addition of conversion noise and laser-induced quasiparticles[3].

In this study, we propose a novel approach for transmitting coherent quantum microwave fields using a room-temperature lossy microwave waveguide. In the proposed scheme, two distant superconducting circuits housed in cryostats are connected by a microwave waveguide that is placed outside the refrigerators and operates at room temperature, as shown in Fig. 1. The principle of operation consists of utilizing a superconducting loop antenna coupled to an  $LC$  harmonic oscillator at the receiving end of the transmission waveguide. According to *Faraday's law* of induction, the loop antenna converts microwave fields to microwave voltages across the  $LC$  harmonic oscillator. Voltages are induced in the  $LC$  oscillator associated with both the transmitted signal and the noise photons. Interestingly, the use of a loop antenna with suitably designed dimensions can significantly suppress the number of induced noise photons in the  $LC$  harmonic oscillator. Additionally, cryogenic preamplification can be used to maintain the signal transmittance at unity. Consequently, we show that near-quantum-limited noise temperature and high-fidelity transmission can be achieved. Hence, the proposed scheme enables the use of a microwave waveguide operating at room temperature to connect two superconducting quantum circuits housed in distant separated cryostats. This approach has the potential to realize a modular superconducting quantum computer (or a local quantum network) without transduction or waveguide cooling. In the remainder of the paper, we develop a theoretical model for the proposed scheme and provide numerical estimates for a typical aluminum waveguide that supports the  $TE_{10}$  fundamental propagation mode.

## II. THEORETICAL MODEL

Consider two separated superconducting quantum nodes (transmitter and a receiver) placed in two distant dilution refrigerators. The two nodes are connected by a nonrefrigerated lossy microwave waveguide. The quantum signal at the transmitter is preamplified at the cryogenic temperature before being launched into the microwave waveguide, as shown in Fig. 1. The preamplifier is coupled to the microwave waveguide with a coupling coefficient of unity, where the waveguide is designed to support the fundamental  $TE_{10}$  mode. Hence, the annihilation operator of the  $TE_{10}$  mode at the input port of the waveguide can be calculated using the following input–output relation [29, 30]:

$$\hat{u} = \sqrt{G}\hat{s} + \sqrt{G}\sqrt{F_a}\hat{f}_s - \hat{f}_w, \quad (1)$$

where  $\hat{u}$  and  $\hat{s}$  are the annihilation operators of the  $TE_{10}$  mode and the source signal at the transmitter,  $G$  and  $F_a$  are the gain and the noise factor of the cryogenic preamplifier, respectively;  $\hat{f}_s$  is the source-generated noise operator; and  $\hat{f}_w$  is the waveguide thermal occupation noise operator. The noise operators are characterized by zero averages  $\langle \hat{f}_s \rangle = \langle \hat{f}_w \rangle = 0$ , and associated noise photons are described by  $N_s = \langle \hat{f}_s^\dagger \hat{f}_s \rangle = \frac{1}{2} \coth(\frac{\hbar\omega}{4\pi k_b T_s})$  [31], and  $N_{th} = \langle \hat{f}_w^\dagger \hat{f}_w \rangle = \frac{1}{\exp(\hbar\omega/k_B T) - 1}$ . Here,  $T_s$  and  $T$  are the cryogenic source temperature and the waveguide room temperature, respectively.

The governing equation of motion of the propagating  $TE_{10}$  mode in the microwave waveguide is given by (see Appendix):  $\frac{\partial \hat{u}(t)}{\partial t} = -\frac{\Gamma}{2}\hat{u}(t) + \sqrt{\Gamma}\hat{f}_L(t)$ , where  $\Gamma$  is the decay coefficient, and  $\hat{f}_L(t)$  is the quantum noise operator, which obeys the relation  $\langle f_L(t_1)^\dagger f_L(t_2) \rangle = N_{th}\delta(t_1 - t_2)$ . The field operator  $\hat{u}(t)$  at the output of the rectangular waveguide can be expressed as:

$$\begin{aligned} \hat{u}(\tau) = & \hat{s}\sqrt{G}e^{-\frac{\Gamma}{2}\tau} + \left( \sqrt{G}\sqrt{F_a}\hat{f}_s - \hat{f}_w \right) e^{-\frac{\Gamma}{2}\tau} \\ & + \sqrt{\Gamma}e^{-\frac{\Gamma}{2}\tau} \int_0^\tau e^{\frac{\Gamma}{2}t} \hat{f}_L(t) dt, \end{aligned} \quad (2)$$

where  $\tau = \frac{l}{v_g}$  is the interaction/propagation time,  $l$  is the waveguide length, and  $v_g$  is the group velocity of the  $TE_{10}$  mode. Note that the noise operators  $\hat{f}_s$ ,  $\hat{f}_w$  and  $\hat{f}_L$  are uncorrelated.

The solution in Eq. 2 can be used in conjunction with the noise properties to determine the number of photons of the  $TE_{10}$  mode at the output of the rectangular waveguide:

$$\begin{aligned} \langle \hat{u}(\tau)^\dagger \hat{u}(\tau) \rangle = & \langle \hat{s}^\dagger \hat{s} \rangle G e^{-\Gamma\tau} + \left( G F_a N_s - N_{th} \right) e^{-\Gamma\tau} \\ & + N_{th}(1 - e^{-\Gamma\tau}). \end{aligned} \quad (3)$$

Here, the first term corresponds to the number of  $TE_{10}$  signal photons, and the second and third terms correspond to the number of noise photons.

We propose the following approach to suppress noise photons and achieve coherent signal transmission. A superconducting loop antenna is used inside the waveguide output port and subjected to the  $TE_{10}$  flux. An  $LC$  harmonic oscillator placed outside the waveguide is coupled to the loop antenna, as schematically demonstrated in Fig. 1. The loop antenna induces a voltage across the coupled  $LC$  harmonic oscillator based on Faraday's law of induction. The antenna and the  $LC$  circuit are designed to suppress the noise photons to the level obtained by a waveguide cooled to the cryogenic temperature. The number of induced photons across the  $LC$  harmonic oscillator can be calculated using the input–output relation and the relation given in (20) (see Appendix), as follows:

$$\begin{aligned} \langle \hat{b}^\dagger \hat{b} \rangle = & \eta G \langle \hat{s}^\dagger \hat{s} \rangle e^{-\Gamma\tau} + \eta \left( GF_a N_s - N_{th} \right) e^{-\Gamma\tau} \\ & + \eta N_{th} (1 - e^{-\Gamma\tau}) + \eta N_{th}, \end{aligned} \quad (4)$$

The first term in Eq. 4 corresponds to the number of induced signal photons (denoted by  $M_s$ ), and the sum of the second and third terms corresponds to the number of induced noise photons (denoted by  $M_n$ ). Here,  $\eta = \frac{C\omega^2\mu_r^2\mu_0^2h_r^2W_r^2}{\frac{1}{2}\Omega^2lWh(\epsilon_0\epsilon_{eff}Z_F^2+\mu_0\mu_r)}$ ,  $C$  is the capacitance, and  $W_r$  and  $h_r$  are the width and height of the loop antenna, respectively. Note that the antenna dimensions are designed to obtain a value for the parameter  $\eta$  that sufficiently suppresses the noise photons, and a cryogenic preamplification gain is provided to maintain the desired number of signal photons.

### III. RESULTS

Cryogenic amplification for the superconducting quantum circuits placed in dilution refrigerators is typically composed of two stages[9]. The first stage is conducted at a cryogenic temperature of a few mK using a travelling wave parametric(TWPA) amplifier. The second stage is conducted at cryogenic temperature of a few K (e.g., 3 K) using a high-electron-mobility transistor (HEMT) amplifier. Considering TWPA and HEMT amplifiers with gains of  $G_T$  and  $G_H$  gain, respectively, and noise factors of  $F_T$  and  $F_H$ , respectively, the total amplification gain is  $G = G_T \cdot G_H$ , and the total noise factor is  $F_a = F_T + \frac{F_H - 1}{G_T}$ . Normally, the noise factors are expressed in terms of the noise temperatures through the relation  $F_j = 1 + \frac{T_j^N}{T_j^I}$ . Here,  $j \in \{T, H\}$  denote the TWPA and HEMT amplifiers,  $T_j^N$  denotes the noise temperature, and  $T_j^I$  denotes the input noise temperature. The input noise temperature of the two amplifiers is  $T_j^I = \frac{\hbar\omega}{4\pi k_b} \coth\left(\frac{\hbar\omega}{4\pi k_b T_j^O}\right)$  [31], where  $T_j^O$  is the corresponding physical operating temperature. The noise temperature of the TWPA amplifier is  $T_T^N = \frac{\hbar\omega}{2\pi k_b} \left( \frac{1}{G_T \ln(1 + \frac{1}{G_T - 1})} - \frac{1}{2} \right)$  [32], whereas the noise temperature of the HEMT amplifier is typically on the order of a few Kelvins. In

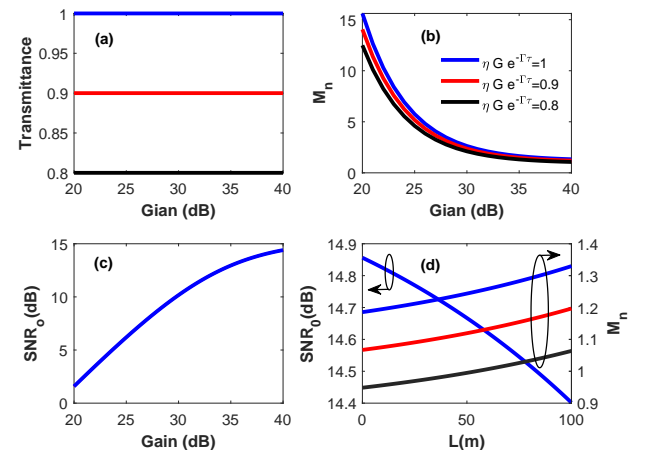


FIG. 2. (a) The signal transmittance versus the gain. Here, the waveguide length  $L = 100$  m. (b) The number of induced noise photons ( $M_n$ ) versus the gain. Here, the waveguide length  $L = 100$  m. Different signal transmittances are considered. (c) The signal-to-noise ratio versus the gain. Here, the waveguide length  $L = 100$  m. (d) The signal-to-noise ratio and the number of induced noise photons ( $M_n$ ) versus the waveguide length. Here, the gain  $G = 40$  dB. Different signal transmittances are considered.

this study, we consider a practical TWPA amplifier with a  $G_T = 10$  dB gain and an operating temperature of  $T_T^O = 20mK$  [31, 32], and an off-the-shelf commercially available HEMT amplifier with a  $G_H = 30$  dB gain, an operating temperature of  $T_H^O = 10K$ , and a noise temperature of  $T_H^N = 4.4K$  [33].

The signal transmittance and the output signal-to-noise ratio (across the  $LC$  harmonic oscillator) can be obtained from Eq. (4), as follows:

$$T_r = \eta G e^{-\Gamma\tau}. \quad (5)$$

$$SNR_o = \frac{\langle \hat{s}^\dagger \hat{s} \rangle}{N_s F_a + 2 \frac{N_{th}}{G} e^{\Gamma\tau}}. \quad (6)$$

Fig. 2 (a) shows the signal transmittance versus the preamplification gain for a waveguide length  $L = 100$  m. The number of noise photons induced across the  $LC$  harmonic oscillator ( $M_n$ ) is shown in Fig. 2 (b). The results show that the transmittance can be maintained close to unity by controlling (increasing) the antenna parameter  $\eta$  for a given gain and waveguide length. However, a larger number of noise photons are induced across the  $LC$  harmonic oscillator. The output signal-to-noise ratio ( $SNR_o$ ) is shown in Fig. 2 (c) for the same parameters and assuming  $\langle \hat{s}^\dagger \hat{s} \rangle = 40$  signal photons. In Fig. 2 (d),  $SNR_o$  and  $M_n$  are plotted versus the waveguide length. Here, the same parameters are assumed for a gain of  $G = 40dB$ . The results show that  $SNR_o$  is independent of the loop antenna parameter  $\eta$  because both the

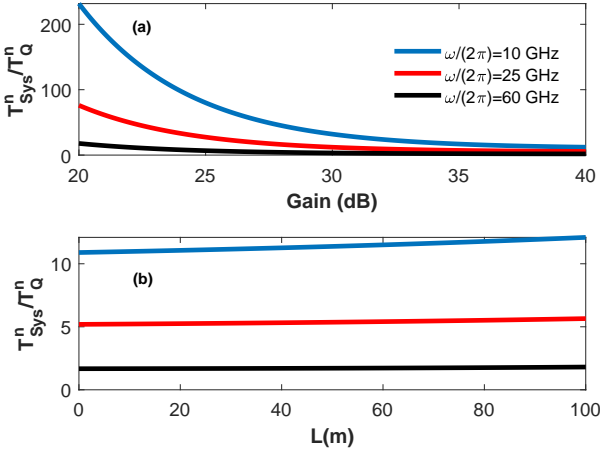


FIG. 3. (a) The normalized system noise temperature (with respect to the quantum-limit noise temperature) versus the gain. Here, the waveguide length  $L = 100$  m, the transmittance  $T_r = 1$ , and three different signal frequencies are considered. (b) The normalized system noise temperature (with respect to the quantum-limit noise temperature) versus the waveguide length. Here, the gain  $G = 40$  dB, the transmittance  $T_r = 1$ , and three different signal frequencies are considered.

signal photons and the induced noise photons are equally scaled by  $\eta$ . However, a larger transmittance (for larger  $\eta$ ) provides a larger number of signal and noise photons.

The performance of the transmission system can be determined by calculating the noise temperature  $T_{Sys}^N$ , as follows:

$$T_{Sys}^N = (F_s - 1)T_{Sys}^I, \quad (7)$$

where  $T_{Sys}^I$  is the input noise temperature of the system (which is equal to the TWPA input noise temperature  $T_T^I$ ), and  $F_s = \frac{SNR_I}{SNR_O} = F_a + \frac{2N_{th}}{GN_s}e^{\Gamma\tau}$  is the system noise factor, where  $SNR_I = \frac{\langle s^\dagger s \rangle}{N_s}$  is the input signal-to-noise ratio at the source.

Fig. 3 shows the system noise temperature (normalized against the quantum-limit noise temperature) versus the waveguide length. Here,  $T_Q^n = \frac{\hbar\omega}{4\pi k_b}$  is the quantum-limit noise temperature. Interestingly, providing proper preamplification and loop antenna design at the receiver results in near-quantum-limited transmission for the proposed system. For instance, the system noise temperature is only 12 times the quantum-limit noise temperature at 10 GHz, and only 1.8 at 60 GHz. This very interesting finding shows the viability of the proposed system as a quantum interconnector.

To further evaluate the system performance, we consider a single quantum bit of information that is generated by the cryogenic source in Fig. 1 and launched toward the room-temperature waveguide for transmission through the proposed system. The generated quantum

state at the source is given by[34, 35]

$$|\psi_s\rangle = a|0\rangle + b\int_{-\infty}^{+\infty} d\omega \xi(\omega)|1_\xi\rangle + \hat{f}_s^\dagger|0\rangle, \quad (8)$$

where  $|0\rangle$  and  $|1_\xi\rangle$  are the vacuum and wave packet states, respectively,  $\xi(\omega)$  is the spectral profile of the generated wave packet, and  $\hat{f}_s$  is the aforementioned source-generated thermal noise. Here,  $\int_{-\infty}^{+\infty} d\omega' \int_{-\infty}^{+\infty} d\omega \xi^*(\omega')\xi(\omega) = 1$  and  $\langle \hat{f}_s \rangle = 0$ .

Hence, the source density matrix  $\rho_s = |\psi_s\rangle\langle\psi_s|$  is given by

$$\begin{aligned} \rho_s = & |a|^2|0\rangle\langle 0| + |b|^2|1_\xi\rangle\langle 1_\xi| + ab^* \int_{-\infty}^{+\infty} d\omega' \xi^*(\omega')|0\rangle\langle 1_\xi| \\ & + ba^* \int_{-\infty}^{+\infty} d\omega \xi(\omega)|1_\xi\rangle\langle 0| + N_s|0\rangle\langle 0|. \end{aligned} \quad (9)$$

Eq.(2), the input-output relation, and Eq.(20) can be used to obtain the output quantum state across the  $LC$  harmonic oscillator as follows:

$$\begin{aligned} |\psi_{LC}\rangle = & a\sqrt{G}\sqrt{\eta}e^{-\frac{\Gamma}{2}\tau}|0\rangle + b\sqrt{G}\sqrt{\eta}e^{-\frac{\Gamma}{2}\tau} \int_{-\infty}^{+\infty} d\omega \xi(\omega)|1_\xi\rangle \\ & + \left( \sqrt{G}\sqrt{F_a} \hat{f}_s^\dagger - \hat{f}_w^\dagger \right) \sqrt{\eta}e^{-\frac{\Gamma}{2}\tau}|0\rangle + \sqrt{\eta}\hat{f}_w^\dagger|0\rangle \\ & + \sqrt{\Gamma}\sqrt{\eta}e^{-\frac{\Gamma}{2}\tau} \left[ \int_0^\tau e^{\frac{\Gamma}{2}t} \hat{f}^\dagger(t)dt \right] |0\rangle. \end{aligned} \quad (10)$$

The first two terms in Eq. (10) correspond to the qubit information generated by the source, the third term corresponds to the source-generated noise, the fourth term corresponds to the thermal occupation noise of the waveguide, and the last term corresponds to the fluctuation-dissipation generated noise.

The output density operator  $\rho_{LC} = |\psi_{LC}\rangle\langle\psi_{LC}|$  is given by:

$$\begin{aligned} \rho_{LC} = & |b|^2 G \eta e^{-\Gamma\tau} |1_\xi\rangle\langle 1_\xi| + |a|^2 G \eta e^{-\Gamma\tau} |0\rangle\langle 0| \\ & + ab^* G \eta e^{-\Gamma\tau} \int_{-\infty}^{+\infty} d\omega' \xi^*(\omega') |0\rangle\langle 1_\xi| \\ & + ba^* G \eta e^{-\Gamma\tau} \int_{-\infty}^{+\infty} d\omega \xi(\omega) |1_\xi\rangle\langle 0| + GF_a N_s \eta e^{-\Gamma\tau} |0\rangle\langle 0| \\ & + \eta N_{th} (1 - e^{-\frac{\Gamma}{2}\tau})^2 |0\rangle\langle 0| + \eta N_{th} (1 - e^{-\Gamma\tau}) |0\rangle\langle 0|. \end{aligned} \quad (11)$$

The closeness of the input and output quantum states in our proposed transmission systems (the pureness of the transmitted state) can be measured by calculating the fidelity  $F$  between the quantum state at the source and the quantum state across the  $LC$  harmonic oscillator at the receiver (which is hereafter referred to as the transmission fidelity) as follows [36]:

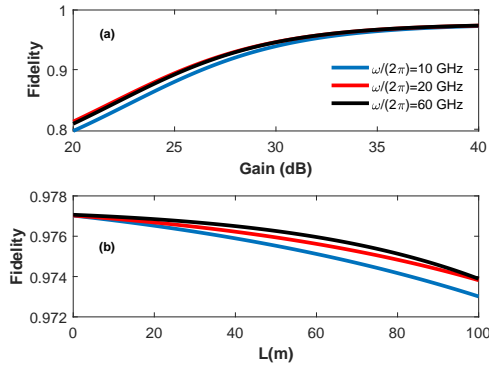


FIG. 4. (a) The transmission fidelity  $F$  versus the gain. A waveguide length  $L = 100$  m and a transmittance of unity are considered. (b) The transmission fidelity  $F$  versus the waveguide length. A gain  $G = 40$  and a transmittance of unity are considered.

$$F = \frac{\text{tr}(\rho_s \rho_{LC})}{\sqrt{\text{tr}(\rho_s^2)} \sqrt{\text{tr}(\rho_{LC}^2)}}, \quad (12)$$

where  $\text{tr}()$  is the trace operator.

Fig. 4 presents the transmission fidelity. Here, a transmittance of unity and three different microwave frequencies are considered. Interestingly, suitable preamplification can produce a fidelity close to unity (greater than 0.97) for waveguide lengths up to one hundred meters. Note that in Fig. 4, the fidelity is independent of the antenna parameter  $\eta$  for a given gain and waveguide length. This result is obtained because decreasing  $\eta$  reduces the number of induced noise photons across the  $LC$  harmonic oscillator, and the transmittance is proportionally reduced in turn, and vice versa. Therefore, transmittance of unity was used to obtain the simulation results in of Fig. 4.

#### IV. DISCUSSION

In quantum microwave transmission systems, the transmission fidelity is severely degraded at room temperature due to significant thermal occupation within the microwave frequency spectrum. Thus, a waveguide cooled to cryogenic temperatures has been proposed to mitigate thermal occupation and achieve acceptable transmission quality. Other techniques, such as implementing controllable coupling between qubits (at the two sides of the link) and the connecting channel, have also been proposed. The potentials and limitations of these techniques were briefly discussed in the introduction.

In this study, we propose a novel technique to effectively cool a waveguide simply by designing a suitable loop antenna at the receiver side, whereby induced thermal noise photons are significantly suppressed. For example, in Fig 4, the thermal waveguide occupation at

room temperature is  $n_{th} = 609$  for a microwave frequency of  $\frac{\omega}{2\pi} = 10$  GHz. However, the number of corresponding induced noise photons across the  $LC$  harmonic oscillator is  $\eta n_{th} = 0.13$ , which is equivalent to that for the same waveguide cooled to 0.255 K. Combining this loop antenna technique with proper cryogenic preamplification results in a room-temperature lossy waveguide with high-fidelity transmission (above 0.97) over significant transmission distances (up to 100 m). To the best of our knowledge, this study is the first proposal of a high-fidelity microwave transmission system using a typical lossy nonrefrigerated waveguide. Our approach has the potential to realize a modular quantum computer with waveguides placed outside dilution refrigerators. This feature is very important because scaling quantum computers up to a capacity of thousands of qubits is crucial for leveraging quantum supremacy. The state-of-the-art capacity of current superconducting quantum computers is less than 127 qubits [17, 23, 37, 38], and boosting the number of qubits to thousands is very challenging, especially from a heat management standpoint. This difficulty is due to the fact that adding a qubit requires connecting a considerable number of cables and related components, which imposes an overwhelming heating load. For example, the estimated cost per qubit to maintain the required cryogenic refrigeration and connect the pertinent cables is approximately \$10 K [39]. Thus, a scaled quantum computer utilizing a giant dilution refrigerator is expected to cost tens of billions of dollars [40]. Connecting separated quantum nodes (or processors) by coherent signaling is a promising approach for efficient scaled quantum computation. The findings reported here have the potential to expedite the realization of sought-after modular superconducting quantum computers capable of containing thousands (million) of qubits. Finally, we note that the proposed scheme (cryogenic preamplification at the transmitter and a passive cryogenic detection circuit at the receiver) is technically very easy to implement.

#### ACKNOWLEDGMENTS

Support for this research was provided by the Abu Dhabi Award for Research Excellence under the auspices of the ASPIRE/Advanced Technology Research Council (AARE19-062) 2019.

#### APPENDIX

Consider a microwave waveguide with a rectangular cross-sectional geometry with a width  $W$  along the  $x$ -axis and a height  $h$  along the  $y$ -axis. The electric and magnetic fields associated with the fundamental  $TE_{10}$  mode of this waveguide can be expressed as follows [41]:

$$\vec{E}(x, y, x, t) = i A Z_F \Omega \sin\left(\frac{\pi x}{W}\right) e^{(i\beta z - \omega t)} \vec{e}_y + \text{c.c.}, \quad (13)$$

$$\vec{H}(x, y, z, t) = -iA\sqrt{\Omega^2 - 1}\sin\left(\frac{\pi x}{W}\right)e^{(i\beta z - \omega t)}\vec{e}_x + A\sqrt{\Omega^2 - 1}\sin\left(\frac{\pi x}{W}\right)e^{(i\beta z - \omega t)}\vec{e}_z + c.c., \quad (14)$$

where  $A$  is the complex amplitude of the  $TE_{10}$  mode,  $Z_F = 377\sqrt{\frac{\mu_r}{\epsilon_r}}$  is the impedance of the filling material, and  $\Omega = \frac{\omega}{\omega_c}$ . Here,  $\omega$  is the microwave signal frequency;  $\omega_c = \frac{2\pi c}{2W\sqrt{\epsilon_r}}$  is the cut-off frequency;  $\mu_r$  and  $\epsilon_r$  are the relative permeability and permittivity of the filling material, respectively;  $\beta$  is a propagation constant; and  $c$  is the speed of light in vacuum. In this study, we consider an aluminum waveguide (with a conductivity  $\sigma = 3.5 \times 10^7 S/m$ ) with a rectangular cross-sectional area of a width  $W = 5$  cm and a height  $h = 2.5$  cm.

### A. Field Quantization

The classical Hamiltonian of the  $TE_{10}$  mode is given by  $\mathcal{H} = \frac{1}{2}\epsilon_0\epsilon_{eff}|A|^2 Z_F^2 \Omega^2 V_{ol} + \frac{1}{2}\mu_0\mu_r|A|^2 \Omega^2 V_{ol}$ , where  $V_{ol} = W \times h \times l$  is the waveguide volume and  $l$  is the waveguide length. The propagating microwave field can be quantized through the following relation:

$$A = \frac{(\hbar\omega)^{\frac{1}{2}}}{\varphi^{\frac{1}{2}}(\epsilon_0\epsilon_{eff}V_{ol})^{\frac{1}{2}}}\hat{a}, \quad (15)$$

where  $\hat{a}$  is the annihilation operator of the  $TE_{10}$  mode,  $\varphi = \frac{\Omega^2 Z_F^2}{2} + \frac{\mu_0\mu_r\Omega^2}{2\epsilon_0\epsilon_{eff}}$ , and  $\epsilon_{eff} = \epsilon_r - \frac{\pi^2 c^2}{W^2 \omega^2}$  is the effective permittivity of the waveguide. Thus, the quantum Hamiltonian is given by  $\hat{\mathcal{H}} = \hbar\omega\hat{a}^\dagger\hat{a}$ . The equation of motion can be obtained by substituting the quantum Hamiltonian into the Heisenberg equation  $\frac{\partial\hat{a}}{\partial t} = \frac{i}{\hbar}[\hat{\mathcal{H}}, \hat{a}]$ . Incorporating the waveguide dissipation and the dissipation-fluctuation noise into this equation, yields  $\frac{\partial\hat{a}}{\partial t} = -i\omega\hat{a} - \frac{\Gamma}{2}\hat{a} + \sqrt{\Gamma}\hat{f}_L$ . Implementing the rotation approximation by setting  $\hat{a} = \hat{u}e^{(-i\omega t)}$  yields the equation of motion as

$$\frac{\partial\hat{u}}{\partial t} = -\frac{\Gamma}{2}\hat{u} + \sqrt{\Gamma}\hat{f}_L, \quad (16)$$

where  $\Gamma = \frac{\alpha}{v_g}$  is the decay time coefficient,  $\alpha = \frac{2R_s}{\sqrt{\mu_0\mu_r}}\frac{\frac{h}{W}(\frac{\omega_r}{\omega})^2 - 1}{\sqrt{1 - (\frac{\omega_r}{\omega})^2}}$  is the attenuation coefficient,  $v_g = c\sqrt{1 - (\frac{\omega_r}{\omega})^2}$  is the group velocity, and  $\hat{f}_L$  is the quantum Langevin noise operator. Here,  $R_s$  is the surface impedance of the waveguide metal material.

### B. Induced Voltage

A superconducting loop antenna with a width  $W_r$  along the  $x$ -axis and a height  $h_r$  along the  $y$ -axis is implemented at the output port of the waveguide and subjected to the  $TE_{10}$  flux. The loop antenna is coupled to an  $LC$  harmonic oscillator. Classically, the induced voltage across the  $LC$  circuit can be described by Faraday's law of induction as follows:

$$V(t) = -\frac{\partial\Psi}{\partial t}, \quad (17)$$

where  $\Psi = \mu_0\mu_r \int_0^{W_r} \int_0^{h_r} \vec{H}(x, y, z, t) \cdot \partial\vec{A}$  is the flux to which the loop antenna is subjected and  $\partial\vec{A} = \partial x \partial y \vec{e}_z$  is the differential element of the enclosed area of the antenna. Thus, the induced voltage across the  $LC$  circuit is given by  $V(t) = V_I e^{-i\omega t + i\beta L} + c.c.$ , where  $V_I$  is the amplitude of the induced voltage and is given by

$$V_I = i\mu_0\mu_r A h_r W_r. \quad (18)$$

The voltage across the  $LC$  circuit can be quantized using the following relation:

$$V_I = \sqrt{\frac{\hbar\omega}{C}}\hat{b}, \quad (19)$$

where  $\hat{b}$  is the annihilation operator of the voltage in the  $LC$  harmonic oscillator;  $C$  is the capacitance, satisfying  $\omega = \frac{1}{\sqrt{LC}}$ ; and  $L$  is the inductance. The quantization relations given in Eq. (15) and Eq. (19) can be used to obtain a direct relation between the annihilation operators of the  $TE_{10}$  mode and the  $LC$  voltage:

$$\hat{b} = i\hat{a}\frac{C^{\frac{1}{2}}}{\varphi^{\frac{1}{2}}(\epsilon_0\epsilon_{eff}V_{ol})^{\frac{1}{2}}}\mu_0\mu_r\omega h_r W_r. \quad (20)$$

where  $\hat{a} = \hat{u}e^{-i\omega t}$ .

---

[1] S. D. et al., A quantum-logic gate between distant quantum-network modules, *Science* **371**, 614 (2021).  
[2] Y. Zhong., Deterministic multi-qubit entanglement in a quantum network, *Nature* **590**, 571 (2021).  
[3] P. M. et al., Microwave quantum link between superconducting circuits housed in spatially separated cryogenic systems, *Phys. Rev. Lett.* **125**, 260502 (2020).  
[4] J. B. et al., On-chip coherent microwave-to-optical transduction mediated by ytterbium in yvo4, *Nat. Commun* **11**, 3266 (2020).  
[5] D. Gottesman and I. Chuang, Demonstrating the viability of universal quantum computation using teleportation and single-qubit operations, *Nature* **402**, 390–393 (1999).

[6] T. Northup and R. Blatt, Quantum information transfer using photons, *Nature Photon* **8**, 356–363 (2014).

[7] L. Jiang, J. Taylor, A. Sørensen, and M. Lukin, Distributed quantum computation based on small quantum registers, *Phys. Rev. A* **76**, 062323 (2007).

[8] C. M. et al., Large-scale modular quantum-computer architecture with atomic memory and photonic interconnects, *Phys. Rev. A* **89**, 022317 (2014).

[9] S. K. et al., Engineering cryogenic setups for 100-qubit scale superconducting circuit systems, *EPJ Quantum Technol* **6** (2019).

[10] T. D. Ladd, F. Jelezko, R. Laflamme, Y. Nakamura, C. Monroe, and J. O'Brien, Quantum computers, *Nature* **464**, 45–53 (2010).

[11] D. A. et al., Development of quantum interconnects (quics) for next-generation information technologies, *PRX Quantum* **2** (2021).

[12] H. J. Kimble, The quantum internet, *Nature* **453**, 1023–1030 (2008).

[13] S. Wehner, D. Elkouss, and R. Hanson, Quantum internet: A vision for the road ahead, *Science* **362** (2018).

[14] L. S. et al., High-rate, high-fidelity entanglement of qubits across an elementary quantum network, *Phys. Rev. Lett.* **124** (2019).

[15] Z. Zhang, S. Mouradian, F. Wong, and J. Shapiro, Entanglement-enhanced sensing in a lossy and noisy environment, *Phys. Rev. Lett.* **114** (2015).

[16] J. Mooij, T. Orlando, L. Levitov, L. Tian, C. van der Wal, and S. Lloyd, Josephson persistent-current qubit, *Science* **285**, 1036 (1999).

[17] F. Arute, K. Arya, R. Babbush, and et al., Quantum supremacy using a programmable superconducting processor, *Nature* **574**, 505–510 (2019).

[18] M. Qasymeh and H. Eleuch, Hybrid two-mode squeezing of microwave and optical fields using optically pumped graphene layers, *Sci. Rep.* **10** (2020).

[19] C. A. et al., On-demand quantum state transfer and entanglement between remote microwave cavity memories, *Nature Phys* **14**, 705–710 (2018).

[20] P. K. et al., Deterministic quantum state transfer and remote entanglement using microwave photons, *Nature* **558**, 264–267 (2018).

[21] Y. Z. et al., Deterministic multi-qubit entanglement in a quantum network, *Nature* **590**, 571–575 (2021).

[22] A. B. et al., Phonon-mediated quantum state transfer and remote qubit entanglement, *Science* **364**, 368 (2019).

[23] J. Gambetta, Ibm's roadmap for scaling quantum technology, IBM Research Blog (2020).

[24] B. Vermersch, P.-O. Guimond, and P. Zoller, Quantum state transfer via noisy photonic and phononic waveguides, *Phys. Rev. Lett* **118** (2017).

[25] Z.-L. Xiang, M. Zhang, L. Jiang, and P. Rabl, Intracity quantum communication via thermal microwave net- works, *Phys. Rev. X* **7** (2017).

[26] M. Qasymeh and H. Eleuch, Quantum microwave-to-optical conversion in electrically driven multilayer graphene, *Opt. Express* **27**, 5945 (2019).

[27] M. Qasymeh and H. Eleuch, Frequency-tunable quantum microwave to optical conversion system, U.S. Patent (2020).

[28] M. Mirhosseini, A. Sipahigil, M. Kalaee, and O. Painter, Superconducting qubit to optical photon transduction, *Nature* **588**, 599–603 (2020).

[29] M. Qasymeh and H. Eleuch, Hybrid two-mode squeezing of microwave and optical fields using optically pumped graphene layers, *Sci Rep* **588** (2020).

[30] C. W. Gardiner and M. J. Collett, Input and output in damped quantum systems: Quantum stochastic differential equations and the master equation, *Phys. Rev. A* **31**, 3761 (1985).

[31] S. S. et al., Characterizing cryogenic amplifiers with a matched temperature-variable, *Review of Scientific Instruments* **92**, 034708 (2021).

[32] L. F. et al., Bimodal approach for noise figures of merit evaluation in quantum-limited josephson traveling wave parametric amplifiers, arXiv:2109.14924v1 (2021).

[33] F. Heinz, F. Thome, A. Leuther, and O. Ambacher, A 50-nm gate-length metamorphic hemt technology optimized for cryogenic ultra-low-noise operation, *IEEE Transactions on Microwave Theory and Techniques* **69**, 3896 (2021).

[34] C. L. M. T. J. Lim and J. Lee, Quantum plasmonics with a metal nanoparticle array, *Phys. Rev. A* **85** (2013).

[35] Z. Y. Ou, Temporal distinguishability of an n-photon state and its characterization by quantum interference, *Phys. Rev. A* **74** (2006).

[36] X. Wang, C.-S. Yu, and X. Yi, An alternative quantum fidelity for mized states of qudits, *Phys. Lett. A* **373**, 58 (2008).

[37] M. G. et al., Quantum walks on a programmable two-dimensional 62-qubit superconducting processor, *Science* **10.1126/science.abg7812** (2021).

[38] B. Yirka, Ibm announces development of 127-qubit quantum processor, *Phys.org* (Nov 16, 2021).

[39] G. Lichfield, Inside the race to build the best quantum computer on earth, *MIT Technology Review* (2021).

[40] J. Levy, 1 million qubit quantum computers: moving beyond the current “brute force” strategy, *SEEQC* (2020).

[41] D. M. Pozar, *Microwave engineering*, John Wiley and Sons (2012).

[42] C. M. et al., A near quantum-limited josephson traveling-wave parametric amplifier, *Science* **350**, 307 (2015).

[43] U. M. et al., Parametric amplification and squeezing with an ac- and dc-voltage biased superconducting junction, *Phys. Rev. Applied* **11**, 034035 (2019).